Radar Imaging Homework 2

Name: Gagan Jattenahalli Harishkumar
Person code: 10881210

January 10, 2026

Introduction

The radar research group has access to two Unmanned Aerial Vehicles (UAVs) equipped with a radar system. The UAVs fly at an approximate height of 60 meters, with a rectilinear trajectory.

The onboard radar system transmits chirp signals modulated around a central/carrier frequency. The received echoes from the targets in the scene are then recorded. Range compression is then performed on the received echoes.

These range-compressed signals are then further processed with a focusing algorithm called Time Domain Back-Projection to obtain an image of the environment.

Acquired Data

The data acquired from the radar system onboard the UAVs are:

- Central/Carrier radar frequency
- Range axis of range-compressed data
- x, y, and z coordinates of the sensor at each slow time τ
- Range-compressed data

Note: slow time (τ) is related to the movement of the platform (UAV). It captures a sample between two consecutive pulses transmitted by the radar.

Range-Compressed Data

The given range-compressed data has a particular format. Each column of the range-compressed data *RCData* consists of exactly one echo signal received by the radar system.

The *RCData* acquired from the radar system consists of the complex echo signals. Individual echo signals present in *RCData* can be depicted as given below:

$$Echo_n{}^T = [a_1 + i * b_1, a_2 + i * b_2, ..., a_{4095} + i * b_{4095}, a_{4096} + i * b_{4096}]$$

The *RCData* composed of about 4000 echo signals and can be represented as given below:

$$RCData = [Echo_1, Echo_2, ..., Echo_{4000}, Echo_{4001}]$$

Note: Each echo signal constitutes one column of RCData.

Range Resolution Assessment

Range resolution of a Synthetic Aperture Radar (SAR) image defines the minimum distance needed between two distinct targets for them to appear as two separate pixels in the SAR image generated from the acquired radar data.

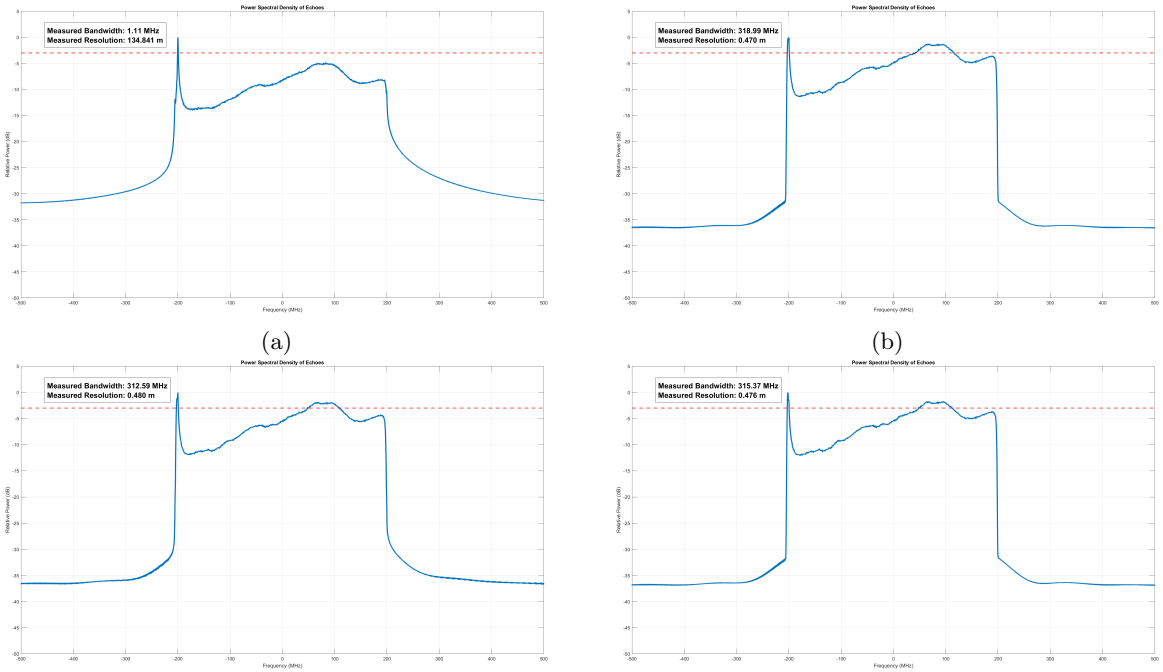

(a) (b) (c) (d)

Figure 1: Variation of calculated bandwidth and range resolution using (a) Rectangular window (b) Hanning window (c) Hamming window (d) Blackman window.

We can compute the range resolution using the acquired radar data.
We know:

$$\text{distance } R = \frac{c * t}{2}; \tag{1}$$

where $c = 3 \times 10^8$ and $t =$ time taken for the pulse to travel to the target and back.

Now, to compute the distance between two distinct targets, we need to compute the time difference between the pulses used to detect these two targets.

$$\Delta R = \frac{c * \Delta\tau}{2}; \tag{2}$$

where $\Delta\tau$ is the time difference of the pulse to travel between the two targets.

We know the minimum distance that can be measured from the radar is given by the inverse of the bandwidth, so we can say:

$$\Delta\tau \approx \frac{1}{B}; \tag{3}$$

where B is the bandwidth of the signal.

So, substituting Eq. 3 in Eq. 2, we get:

$$\Delta R = \frac{c}{2 * B}; \tag{4}$$

Calculate Bandwidth from the Data

The bandwidth of a given signal can be calculated from the Power Spectral Density (PSD) of the signal. Based on the point of measurement, the measured bandwidth can vary.

Some of the points where the bandwidth of the radar can be measured are: 3dB below the peak power, 6dB below the peak power, 10dB below the peak power, and 20dB below the peak power.

The common reasons for the use of the above-mentioned points are:

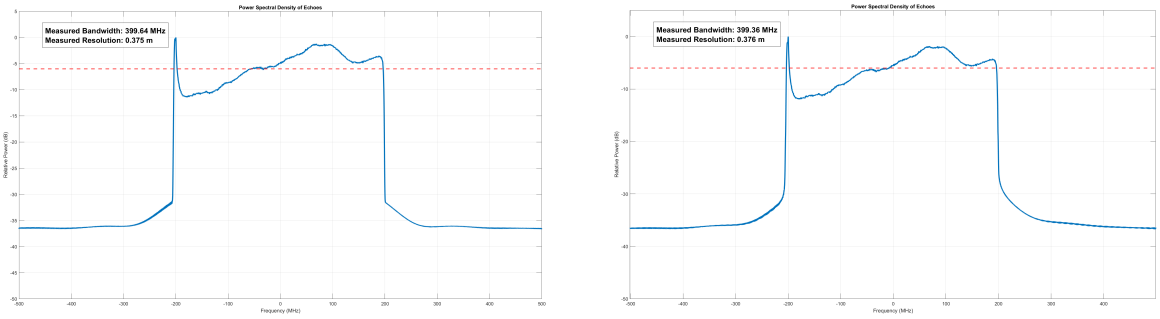

(a) (b)

Figure 2: Variation of calculated bandwidth and range resolution using (a) Hanning window (b) Hamming window with crossover point as 6dB below the peak power.

- -3dB: The power ratio at 3dB below peak power is 50% of the total power. So, for the calculation of range resolution, we would have to use this.
- -6dB: Often used when analyzing signals with Hamming or Hanning windows, as their crossover points often sit naturally at -6dB.
- -10dB: Common in antenna engineering to define "usable" bandwidth or where an antenna starts to become inefficient.
- -20dB: Used to define where the signal "ends" and the noise/interference begins.

The measured bandwidth also varies with the windowing method used. The industry-standard windowing method used is the Hamming window. The effects of various windowing methods on the measured bandwidth and range resolution can be seen in Fig. 1.

The crossover point for Hamming and Hanning windows is -6dB, the resulting bandwidth and range resolution measurements for which are shown in Fig. 2. The range resolution and bandwidth measured using Hamming and Hanning windows at 6dB below peak power is the closest to the theoretical bandwidth and range resolution of the system.

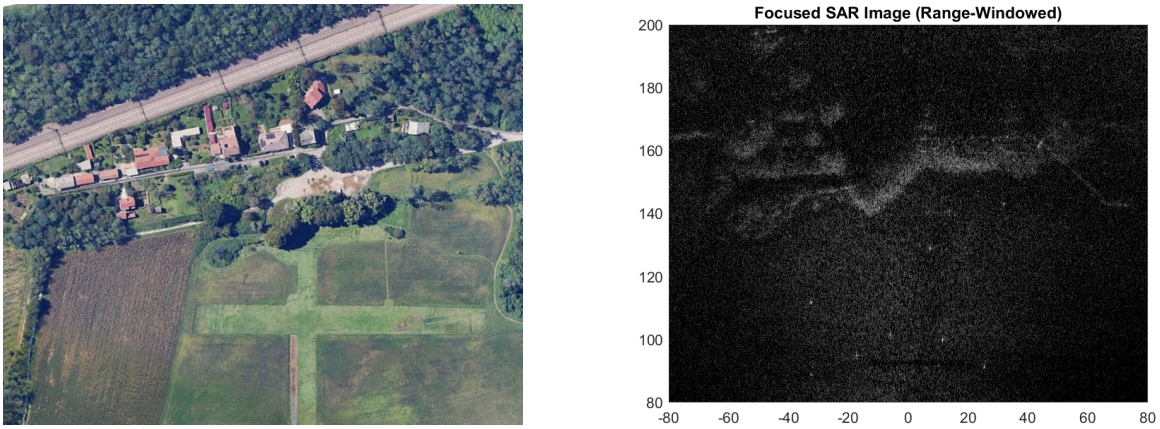

(a) Optical Reference (b) TDBP SAR Image

Figure 3: Comparison between optical and radar imaging.

Time Domain Back-Projection

Time Domain Back-Projection is an algorithm that is used to generate a SAR image from the radar data. The data contains information about the x-axis range and y-axis range.

$$x \in [-80, 80] \qquad y \in [80, 200]$$

The algorithm to generate the image using the TDBP algorithm is given in algorithm 1.

Algorithm 1 Time Domain Back-Projection (TDBP)

Step 1: Grid Generation
Create vectors $x = [-80 : \Delta x : 80]$ and $y = [80 : \Delta y : 200]$
$[X, Y] \leftarrow \text{meshgrid}(x, y)$
$Z \leftarrow \text{zeros}(\text{size}(X))$
$I \leftarrow \text{zeros}(\text{size}(X))$ ▷ Pre-allocate SAR Image
Step 2: Back-Projection Loop
for $i = 1$ **to** N_{echoes} **do**
    $R \leftarrow \sqrt{(X - S_x(i))^2 + (Y - S_y(i))^2 + (Z - S_z(i))^2}$
    $S \leftarrow \text{interp1}(r_{ax}, RCData(:, i), R)$ ▷ Interpolate Echo
    $S_{rephased} \leftarrow S \cdot \exp\left(j \frac{4\pi}{\lambda} R\right)$ ▷ Apply Phase Term
    $I \leftarrow I + S_{rephased}$ ▷ Coherent Accumulation
end for
Step 3: Visualization
Plot $|I|$ using `imagesc`

The image generated using the TDBP algorithm and the optical image of the generated SAR image, for reference, are shown in Fig. 3.

De-Speckling

In order to get rid of the noise present in the SAR image, we can perform a de-speckling operation on the SAR image. This is done by performing a moving average over the image.

A comparison between the effects of different kernel sizes is also performed. The kernels are such that all the values in the kernel are N^{-2}, where N is the size of the kernel.

To perform de-speckling, a 2D convolution of the image with the kernel is performed. The results thus obtained are shown in Fig. 4.

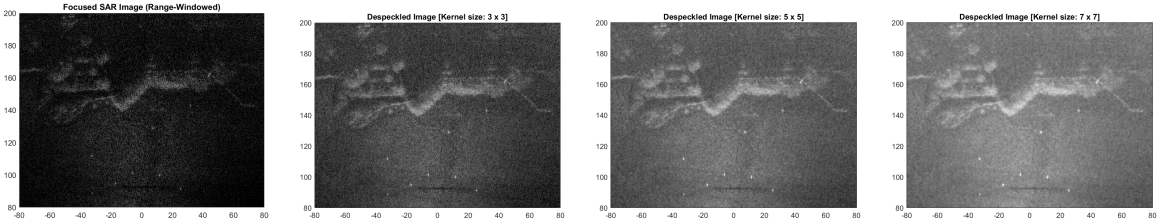

(a) (b) (c) (d)

Figure 4: (a) SAR image and de-speckling with (b) 3×3 kernel (c) 5×5 kernel (d) 7×7 kernel.

Resolution Assessment using Corner Reflectors

To verify imaging performance, a high-resolution patch was focused around a corner reflector at $(-6, 101)$ m. A focused point target represents the system's Impulse Response Function (IRF). Theoretically, range resolution is defined by the bandwidth B:

$$\Delta R \approx \frac{c}{2B} \tag{5}$$

Resolution was assessed by applying a 2D Fast Fourier Transform (FFT) to the complex patch to observe its spatial frequency support. As shown in Figure 5, the sinc-like spatial response corresponds to a rectangular "bandwidth box" in k-space. The resolution is inversely proportional to the spectral width:

$$\delta_y = \frac{1}{\Delta k_y}, \quad \delta_x = \frac{1}{\Delta k_x} \tag{6}$$

The sharp rectangular boundaries in the frequency domain confirm that the TDBP algorithm correctly preserved the phase and frequency content, with measured values aligning with theoretical limits.

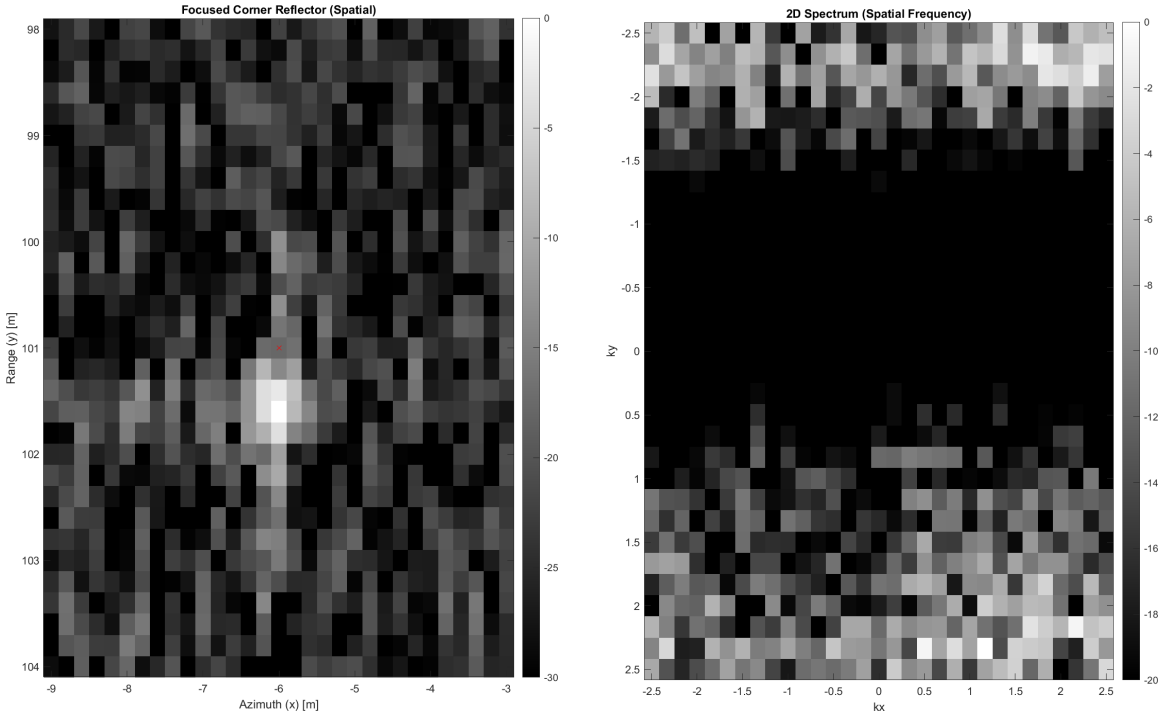

(a) Focused Patch (Spatial Domain) (b) 2D Spectrum (Frequency Domain)

Figure 5: Resolution assessment of the corner reflector at $(-6, 101)$ m. The left image shows the spatial IRF, while the right image shows the FFT of the zoomed-in image of the corner reflector.

The Effects of Trajectory Errors

Trajectory errors are one of the most common types of errors encountered during acquisition of data using UAVs. It can be very insightful to understand how these kinds of errors affect the SAR image.

The change in the SAR image due to the errors depends on how extreme the standard deviation is with respect to the wavelength of the radar. Figures 7, 8, 9, and 10 show the data acquired by the UAVs, the noise added to the position parameters, and the results of it.

The effects of the noise on the SAR image are visualized in Fig. 6.

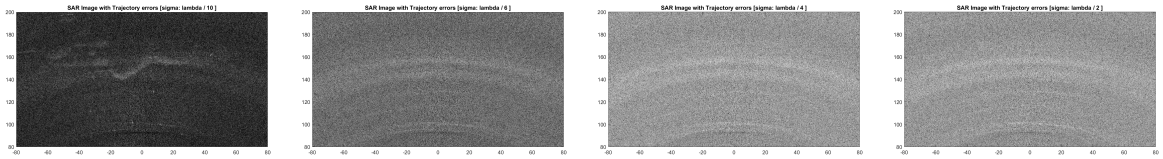

(a) (b) (c) (d)

Figure 6: Effects of noise with standard deviation of (a) $\lambda/10$ (b) $\lambda/6$ (c) $\lambda/4$ (d) $\lambda/2$.

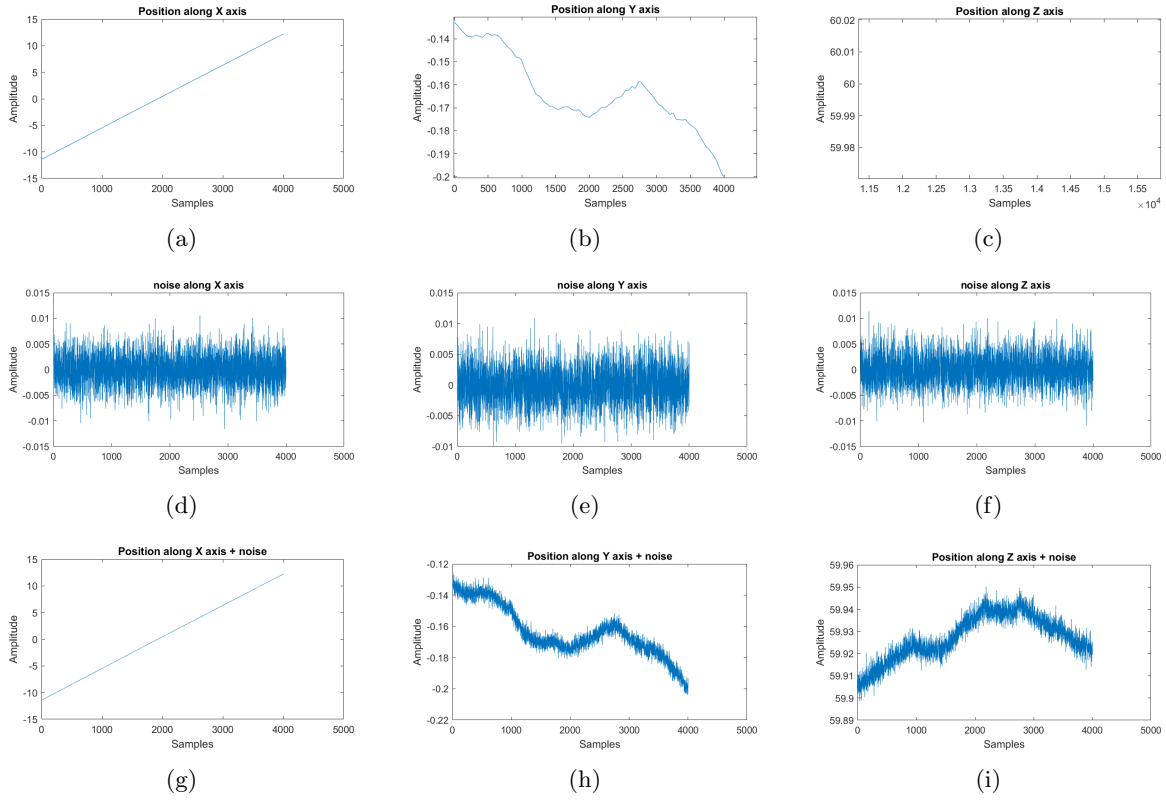

Figure 7: Trajectory Analysis: (a) (b) (c) acquired X, Y, and Z coordinate data, (d) (e) (f) noise residuals, (g) (h) (i) and noisy trajectory (bottom) for $\sigma = \lambda/10$.

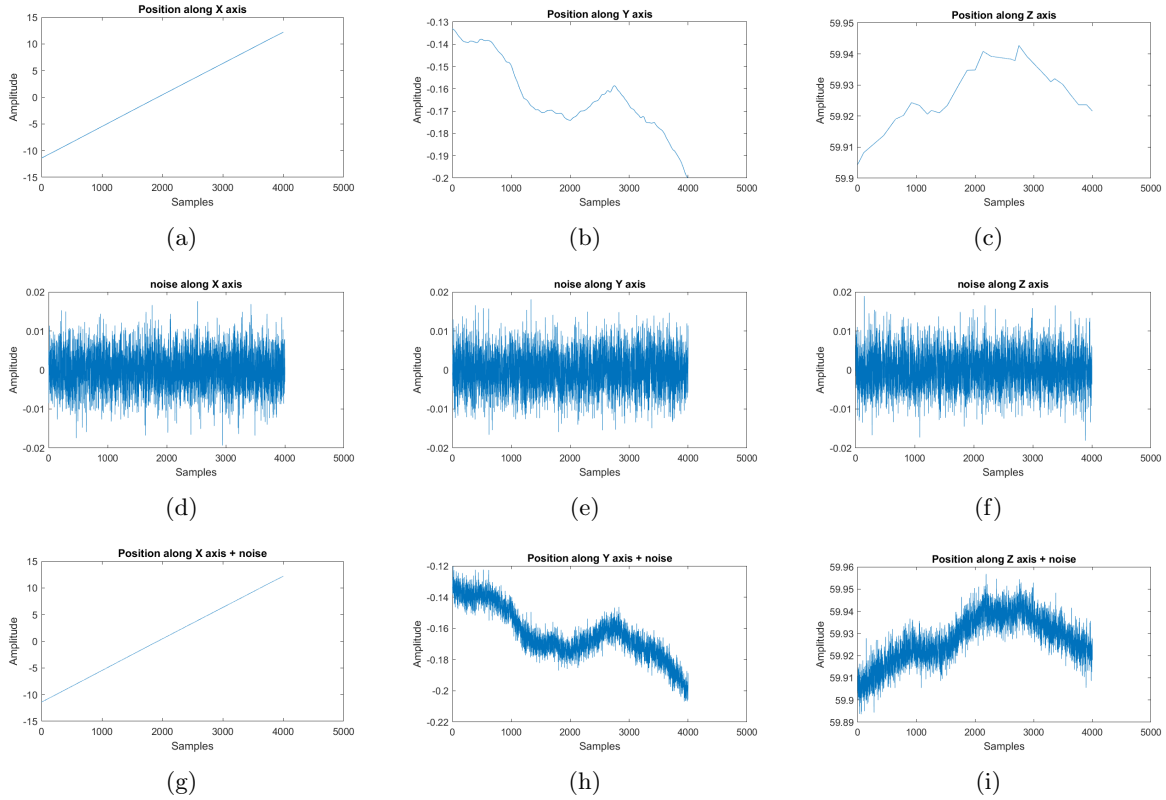

Figure 8: Trajectory Analysis: (a) (b) (c) acquired X, Y, and Z coordinate data, (d) (e) (f) noise residuals, (g) (h) (i) and noisy trajectory (bottom) for $\sigma = \lambda/6$.

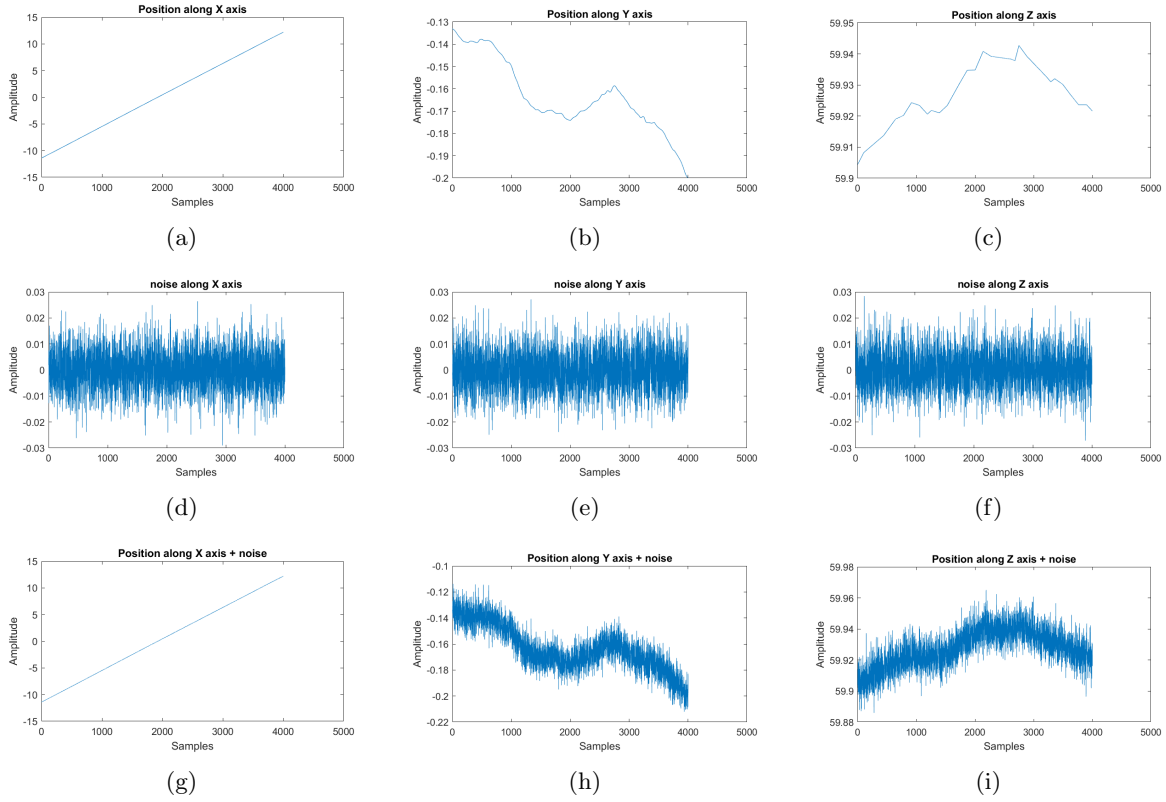

Figure 9: Trajectory Analysis: (a) (b) (c) acquired X, Y, and Z coordinate data, (d) (e) (f) noise residuals, (g) (h) (i) and noisy trajectory (bottom) for $\sigma = \lambda/4$.

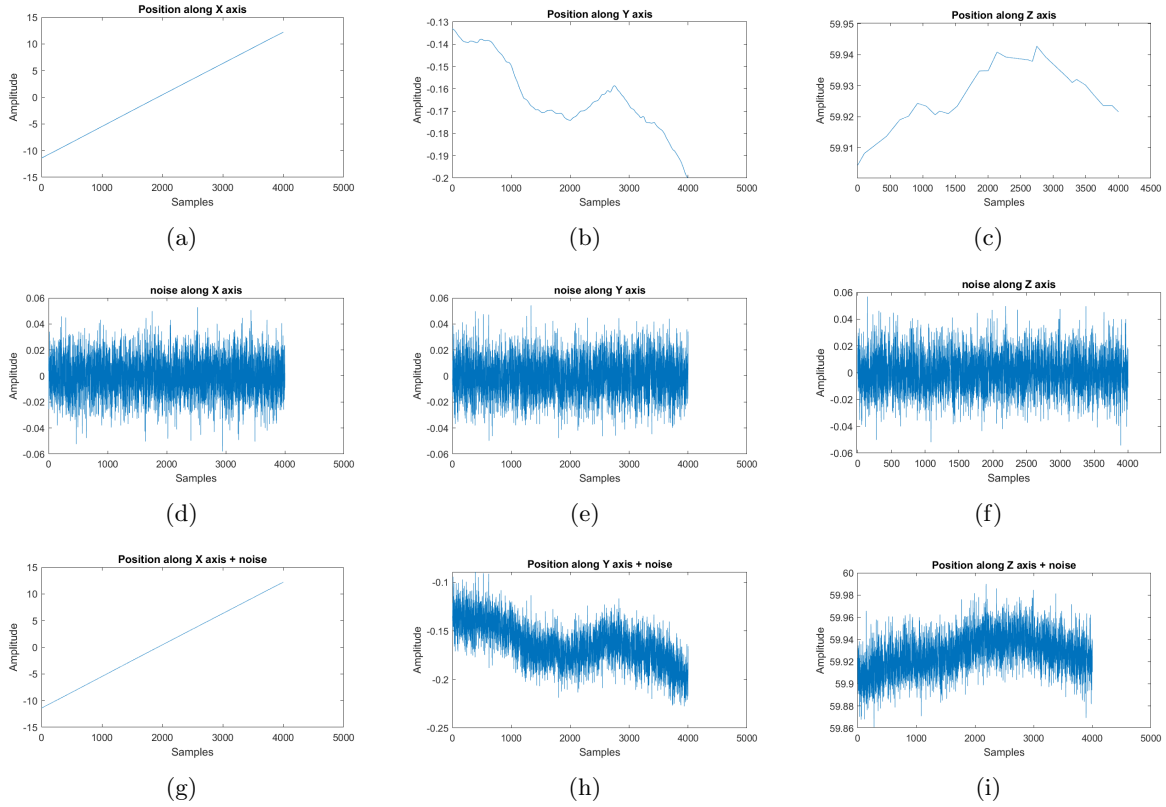

Figure 10: Trajectory Analysis: (a) (b) (c) acquired X, Y, and Z coordinate data, (d) (e) (f) noise residuals, (g) (h) (i) and noisy trajectory (bottom) for $\sigma = \lambda/2$.